




METHOD

Inducible and tissue-specific cell labeling in *Cre-ER^{T2}* transgenic *Xenopus* linesTzi-Yang Lin^{1,2}  | Yuka Taniguchi-Sugiura¹ | Prayag Murawala^{1,3,4}  | Sarah Hermann⁵ | Elly M. Tanaka¹ ¹Research Institute of Molecular Pathology (IMP), Vienna BioCenter (VBC), Vienna, Austria²Vienna BioCenter PhD Program, Doctoral School of the University of Vienna and Medical University of Vienna, Vienna, Austria³MDI Biological Laboratory, Bar Harbor, Maine, USA⁴Clinic for Kidney and Hypertension Diseases, Hannover Medical School, Hannover, Germany⁵DFG Research Center for Regenerative Therapies, Technische Universität Dresden, Dresden, Germany

Correspondence

Elly M. Tanaka, Research Institute of Molecular Pathology (IMP), Vienna BioCenter (VBC), 1030 Vienna, Austria.
Email: elly.tanaka@imp.ac.at

Funding information

E.M.T. was supported by core funds of the I.M.P., DFG FZT 111, and ERC AdG 294324 RegenerateAcross, and 742046 RegGeneMems.

Communicating Editor: Haruki Ochi

Abstract

Investigating cell lineage requires genetic tools that label cells in a temporal and tissue-specific manner. The bacteriophage-derived *Cre-ER^{T2}/loxP* system has been developed as a genetic tool for lineage tracing in many organisms. We recently reported a stable transgenic *Xenopus* line with a *Cre-ER^{T2}/loxP* system driven by the mouse *Prrx1* (*mPrrx1*) enhancer to trace limb fibroblasts during the regeneration process (*Prrx1:CreER* line). Here we describe the detailed technological development and characterization of such line. Transgenic lines carrying a CAG promoter-driven *Cre-ER^{T2}/loxP* system showed conditional labeling of muscle, epidermal, and interstitial cells in both the tadpole tail and the froglet leg upon 4-hydroxytamoxifen (4OHT) treatment. We further improved the labeling efficiency in the *Prrx1:CreER* lines from 12.0% to 32.9% using the optimized 4OHT treatment regime. Careful histological examination showed that *Prrx1:CreER* lines also sparsely labeled cells in the brain, spinal cord, head dermis, and fibroblasts in the tail. This work provides the first demonstration of conditional, tissue-specific cell labeling with the *Cre-ER^{T2}/loxP* system in stable transgenic *Xenopus* lines.

KEYWORDS

Cre-ER^{T2}/loxP, fibroblast, inducible cell labeling, *Xenopus laevis*

1 | INTRODUCTION

The ability to label cells and unambiguously trace their progenies provides valuable insights into the cellular mechanisms during development and regeneration. To achieve this, a specific cell type of interests has to be permanently labeled to allow detection at later time points. In addition, temporal labeling is required to obtain unambiguous lineage tracing results. The latter is especially crucial because many developmental genes are re-activated during regeneration, leading to potential

new labeling of cells if the labeling system is not temporally controlled. Another important point to consider is that regeneration studies usually focus on adult tissues, so that such lineage tracing system must be integrated into the genome as a stable transgenic line to enable labeling at the late development and adult stages.

The bacteriophage-derived *Cre-ER^{T2}/loxP* system is the most commonly used lineage tracing system. It was first developed in mammalian cell lines (Feil et al., 1997). The Cre recombinase is fused to the mutated ligand binding domain of the human estrogen receptor (*ER^{T2}*), which prevents the recombinase from entering the nucleus by binding to the heat shock protein hsp90. Upon

This article is part of the special issue "Versatile utilities of amphibians".

This is an open access article under the terms of the [Creative Commons Attribution-NonCommercial-NoDerivs](https://creativecommons.org/licenses/by-nc-nd/4.0/) License, which permits use and distribution in any medium, provided the original work is properly cited, the use is non-commercial and no modifications or adaptations are made.

© 2022 The Authors. *Development, Growth & Differentiation* published by John Wiley & Sons Australia, Ltd on behalf of Japanese Society of Developmental Biologists.

binding to 4-hydroxytamoxifen (4OHT), ER^{T2} releases hsp90, allowing the recombinase to enter the nucleus to recombine *loxP* sites on the reporter cassette. This method was further established in vivo in mice (Metzger & Chambon, 2001) and has been adopted in multiple organisms, including zebrafish (Hans et al., 2009) and axolotls (Khattak et al., 2013). However, this approach has not resulted in stable transgenic lines in *Xenopus laevis* despite its utility in developmental research. One attempt to utilize the *Cre-ER^{T2}/loxP* system to trace the limb muscle cell lineage resulted in very few labeled muscle cells and the line was determined unsuitable for lineage tracing (Rodrigues et al., 2012).

We recently reported a stable transgenic *Xenopus* line that harbors the *Cre-ER^{T2}/loxP* system to investigate the contribution of the fibroblast lineage during *Xenopus* limb regeneration using the mouse *Prrx1* (*mPrrx1*) enhancer (*Prrx1:CreER* line, Lin et al., 2021). Subsequent isolation and sequencing of the labeled fibroblasts further revealed the molecular progression of fibroblasts during limb regeneration. Here we present the entire development of our transgenic *Xenopus* lines harnessing the *Cre-ER^{T2}/loxP*-based lineage tracing method. We first report the proof-of-principle *ER^{T2}-Cre-ER^{T2}* transgenic lines driven by the CAG promoter (referred to as *CAGWGs:ERCReER* in this study). Despite having a lower transgenic efficiency, *CAGGs:ERCReER* lines showed conditional labeling of the tadpole tail when treated with 4OHT at metamorphosis onset. Notably, leg tissues were labeled only with post-metamorphic, but not pre-metamorphic 4OHT treatment, indicating that the treatment timing was crucial for optimal cell labeling. We then further determined the optimal 4OHT treatment regime for our *Prrx1:CreER* lines and improved the labeling efficiency in the limb bud from 12.0% to 32.9%. Detailed immunohistochemistry (IHC) characterization showed that the new 4OHT treatment regime labeled limb bud mesenchyme cells, as well as some cells in the brain, heart, tail dermis, and spinal cord to a lesser extent. Importantly, single *ER^{T2}* *CAGGs* lines (*CAGGs:CreER*) showed 4OHT-independent labeling, while double *ER^{T2}* *Prrx1* lines (*Prrx1:ERCReER*) showed very low labeling efficiency. We hope that our discovery could serve as a reference for the *Xenopus* research community and benefit the future development of lineage tracing techniques in *X. laevis*.

2 | MATERIALS AND METHODS

2.1 | Animal husbandry

Wild-type *X. laevis* were obtained from the European *Xenopus* Resource Center, UK and NASCO, USA, and were maintained in CRTD and IMP animal facilities. Transgenic lines were generated in the CRTD facility and maintained in CRTD and IMP facilities, in which the temperature was 19–20°C. All animal handling procedures were carried out as described in (Sive et al., 2000) and (Lin et al., 2021) and in accordance with local ethics committee guidelines. Animal experiments were performed as approved by the State Authorities Saxony and the Magistrate of Vienna. To obtain embryos from natural mating, a female and a male of chosen genotype were injected with 500 IU and 50 UI of human chorionic gonadotropin (hCG, Sigma-Aldrich, CG10), respectively. The pair

were then put together in 7 L 20 mM NaCl at room temperature overnight. The embryos were collected for the next 2 days before the mating pair was separated. To obtain frog eggs for transgenesis, wild-type females were primed with 50 IU of pregnant mare serum gonadotropin (PMSG, ProSpec, HOR-272) 1 week before the injection of 500 IU of hCG (Sigma-Aldrich, CG10) in the evening before egg collection. Depending on the developmental stages, animals were anesthetized in 0.01%–0.003% benzocaine (Sigma-Aldrich, E1501) before inspection under a stereoscope (Olympus SZX16).

2.2 | Plasmid construction

The CAG promoter was cloned upstream of the *TFPnl5-T2A-ER^{T2}-Cre-ER^{T2}* and *TFPnl5-T2A-ER^{T2}-Cre-ER^{T2}* cassettes in the same fashion as described in (Gerber et al., 2018). *TFPnl5* represents the DNA sequence of a nuclear localization signal (*nls*) fused with the teal fluorescent protein gene *mTFP1* described previously (Ai & Campbell, 2008). The resulting construct *CAG:TFPnl5-T2A-ER^{T2}-Cre-ER^{T2}* was termed the *CAGGs:ERCReER* plasmid in the current study. The construction of *Prrx1:CreER* and *CAGGs:lp-Cherry* (*CAG:(loxP)eGFP* (*loxP*)/*mCherry*) plasmids was described in (Lin et al., 2021). In brief, the original *TFPnl5-T2A-ER^{T2}-Cre-ER^{T2}* cassette in the *mPrrx1:TFPnl5-T2A-ER^{T2}-Cre-ER^{T2}* plasmid was replaced with a codon-optimized version (GeneArt) using restriction enzymes *NheI* and *EcoRI*. The *cryg1:mCherry* cassette (*X. laevis* γ -*crystallin* promoter, *mCherry*, and *SV40 poly-A* sequences) was assembled using overextension PCR before being subcloned into the *mPrrx1:TFPnl5-T2A-ER^{T2}-Cre-ER^{T2}* construct using restriction enzymes *Apal* and *MluI*. The new construct *cryg1:mCherry;mPrrx1:TFPnl5-T2A-ER^{T2}-Cre-ER^{T2}* was termed the *Prrx1:CreER* plasmid in the current study. The *CAGGs:Stop-lp-Cherry* (*CAG:loxP-Stop-loxP-mCherry*) plasmid was made by replacing the *eGFP* sequence of the *CAGGs:lp-Cherry* plasmid with a *TAATTAATTAA* sequence. All plasmids used in transgenesis were prepared with the QIAGEN Maxi kit (Qiagen, 12163).

2.3 | Transgenesis, screening, and 4-hydroxytamoxifen (4OHT) treatment

All transgenic *X. laevis* lines were established based on the REMI protocol (Kroll & Amaya, 1996) and described in (Lin et al., 2021). Specifically, freshly collected wild-type eggs were dejellied using 2% L-cysteine pH 7.8 (Sigma-Aldrich, C126) and aligned on a 2% agarose mold filled with 0.4× MMR/5% ficoll (GE Healthcare, 17-0300-50). To prepare the injection solution, 2 μ l purified plasmid (300–600 ng in total) was incubated with 4 μ l wild-type sperm nuclei (4×10^5 nuclei) for 5 min at room temperature before 18 μ l SDB, 2 μ l egg extract, 2 μ l 100 mM MgCl₂, and 1 μ l I-SceI enzyme (NEB, R0694L, 1:10 diluted) were added to the mixture. After 15 min, 5 μ l of the new mixture was mixed with 150 μ l SDB buffer and back loaded into a glass needle with a 40–60-mm opening. The needle was connected to an infusion pump (World Precision Instruments, SP100i) with a flow rate of 0.6 nL/second. Around 5–10 nL of the plasmid/nuclei mixture was

injected into each egg. The injected eggs were kept in $0.1\times$ MMR at 16°C overnight before being transferred to fresh $0.1\times$ MMR. The MMR solution was refreshed daily until day 5 when surviving embryos that developed normally were counted.

To generate the CAGGs:*ERC*CreER founders, the CAGGs:*ERC*CreER and CAGGs:*Stop-lp-Cherry* plasmids were mixed at a 1:1 ratio and co-injected following the REMI protocol. The surviving embryos were screened at stage 49 (around 30 days old) using the nuclear TFP signal. The transgenesis efficiency was calculated as the number of TFP-positive animals divided by the total number of surviving animals at day 5. To induce the recombination of *loxP* reporter cassettes, TFP-positive animals were bathed in $1\ \mu\text{M}$ 4OHT/ $0.1\times$ MMR or DMSO/ $0.1\times$ MMR overnight and screened for mCherry expression 5–7 days later. Three independent CAGGs:*ERC*CreER founders were kept until sexual maturity and their TFP-positive offspring were screened in a similar fashion as described above. The CAGGs:*Stop-lp-Cherry* cassette was not excluded when screening under the microscope. The F1 transgenic lines (*Xla.Tg* (CAG:TFPnl, *ER*^{T2}-*Cre-ER*^{T2}; CAG:mCherry)^{Tanaka}) are termed CAGGs:*ERC*CreER lines in the current study.

To identify the *Prrx1:CreER* founders, mCherry fluorescence signals in the lens were screened 7 days after transgenesis. Eleven founders were obtained, kept, and mated with the CAGGs:*lp-Cherry* reporter lines (*Xla.Tg*(CAG:eGFP,mCherry)^{Tanaka}). The animals were screened for lens mCherry and trunk GFP fluorescence signals at day 7. Lens-Cherry/trunk-GFP-double positive animals were then bathed in $1\ \mu\text{M}$ 4OHT overnight for specific periods as illustrated in Figure 3B and Figure S3B. mCherry expression in the hindlimb bud was checked at least 1 week after the last 4OHT treatment or at the specific time point indicated in Figure 3B and Figure S3C. The F1 transgenic lines (*Xla.Tg*(*cryg1:mCherry*; *Mmu.Prrx1:TFPnl, Cre-ER*^{T2})^{Tanaka}) are termed *Prrx1:CreER* lines in the current study.

2.4 | Genotyping

Tadpole tail tissues were collected by tail clipping and lysed for 5–10 min at 95°C in $100\ \mu\text{l}$ $50\ \text{mM}$ NaOH. After cooling down to room temperature, $10\ \mu\text{l}$ of $1\ \text{M}$ Tris pH 8 was added to the solution to neutralize the pH. The crude tissue lysates were diluted 10 times before using them as the template input of PCR reactions. The primers used in this study were: *Stop-lp-Cherry*: forward: 5'-TTCGGCTTCTGGCGTGTGAC-3' (on the CAG promoter), reverse: 5'-TTATCCTGCATCGACCTAGACTAG-3' (before the second *loxP* site); *CreER*: forward: 5'-CAACGAGTGATGAGGTTCGCAAG-3', reverse: 5'-TTGGTCCAGCCACCAGCTTG-3'; *GFP*: forward: 5'-GCGACGTAAACGGCCACAAG-3', reverse: 5'-TCGTCCATGCCGAGATGATC-3'. The PCR products were separated by electrophoresis and visualized using a ChemiDoc MP imaging system (Bio-Rad, 12003154).

2.5 | In vivo imaging

To check the developmental stages and the fluorescence signals, an anesthetized animal was loosely wrapped with a piece of kimwipe

(Kimtech Science, 7551) and placed on a 100-mm dish. The kimwipe was used to keep the animal moist and to hold the animal in a certain position so that the tissue region of interest was facing upward. Ring forceps were used to handle the animal and the kimwipe. The dish was then placed under a dissecting microscope setup (Olympus SZX16 with a Zyla 5.5 sCMOS camera and an X-Cite Xylis Broad Spectrum LED Illumination System as the fluorescence light source). Metamorph (MetaMorph Microscopy Automation and Image Analysis Software [RRID:SCR_002368]) was used to capture the images.

2.6 | Immunohistochemistry and microscopy

Animals were sacrificed before tissue collection. Tissues of interest were dissected under a dissecting microscope (Olympus SZX10) and fixed overnight in 4% MEMFA ($1\times$ MEM [41.86 g MOPS, 0.5 g $\text{MgSO}_4\cdot 7\text{H}_2\text{O}$, 1.52 g EGTA, dissolve in H_2O and fill up to 200 ml, pH 7.4], 3.7% formaldehyde [Sigma-Aldrich, 1040031000]) on a rotor in a cold room overnight. Samples were washed three times in PBS and incubated with 30% sucrose overnight in the cold room. An additional overnight decalcification step using 8% EDTA/PBS was performed after the fixation step when preparing stage 66 leg samples. After the sucrose treatment, samples were washed three times in $1\times$ PBS and embedded as OCT blocks ready for cryosection and further analysis. The OCT blocks were cut into 8-mm sections, which were collected on loading slides with a cryostat (NX70, Thermo Scientific). Cryosections were dried and stored in -20°C . Before immunostaining, slides were thawed and stained with primary antibodies against GFP (Rockland, 600-401-215, 1:1000, and MPI-CBG, Dresden, 1:1000), mCherry (Acris Antibodies, AB0040-200, 1:1000), *Prrx1* (Gerber et al., 2018, 1:200), MHC (Developmental Studies Hybridoma Bank, A4.1025, 1:200), and *Sox2* (Mchedlishvili 2012, 1:2000). Alexa 488-, Alexa 568-, and Alexa 647-conjugated antibodies (Invitrogen, 1:500) were used as secondary antibodies. All sections were stained with DAPI (Sigma-Aldrich, D9542, 1:1000) and mounted in Mowiol 4-88/DABCO mounting medium (Sigma-Aldrich, 9002-89-5). Images were taken using a Zeiss Axio Imager Z2 (upright) with an sCMOS camera. The ratio between the number of Cherry-positive cells and the total number of limb bud mesenchymal cells was calculated as the conversion efficiency. At least three sections of each sample were counted using ZEN Blue software. Statistical analysis was done using Prism 9.0.2 (GraphPad Software).

3 | RESULTS

3.1 | Conditional labeling of tail tissues in F0 *X. laevis* carrying an *ER*^{T2}-*Cre-ER*^{T2}/*loxP* system driven by the CAG promoter

To investigate whether 4OHT-induced cell labeling could be robustly achieved in tadpole stages, we performed REMI transgenesis using

both *Cre-ER^{T2}* and *loxP* reporter plasmids (Figure 1A) (see Section 2 for details). The CAG promoter was used to drive the pan-expression of the *ER^{T2}-Cre-ER^{T2}* cassette (CAG:*TFPnl*s-T2A-*ER^{T2}-Cre-ER^{T2}*, abbreviated as the CAGGs:*ERCreER* plasmid), which included an *mTFP1* sequence (Ai & Campbell, 2008) fused with a nuclear localization signal (*nls*) sequence as a screening marker. The *loxP* reporter plasmid was designed to have a floxed stop codon plus a triple *SV40 poly-A* sequence, with an *mCherry* sequence at the second position (CAG:*loxP-Stop-3xSV40pA-loxP-mCherry*, abbreviated as CAGGs:*Stop-lp-Cherry*). The CAGGs:*ERCreER* and CAGGs:*Stop-lp-Cherry* plasmids were mixed and used for transgenesis. The surviving F0 embryos were kept

until stage 49 (Nieuwkoop & Faber, 1956) when we screened for nuclear TFP expression in the tail (Figure 1B). A low efficiency (TFP-positive divided by total surviving embryos) was observed. From four batches of REMI experiments, eight TFP-positive tadpoles out of 172 surviving embryos were obtained (Figure 1A). The average efficiency of the experiments using the CAGGs:*ERCreER* plasmid (4.9%) was significantly lower compared to the efficiency of the experiments using the CAGGs:*TFPnl*s plasmid (71.8%) (Figure 1C). The low transgenesis efficiency is likely due to the increased cassette length, as we observed a negative correlation between transgenic efficiency and the length of DNA cassettes (Figure S1A). Despite having such a

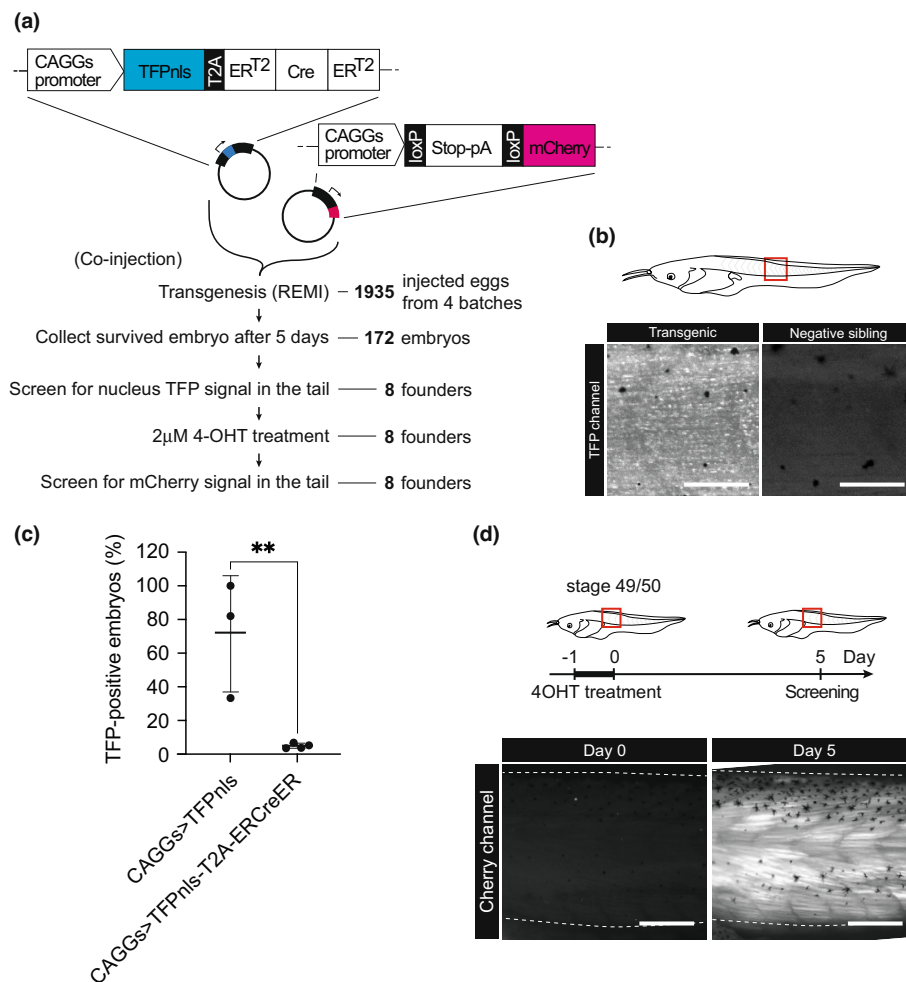


FIGURE 1 Conditional labeling of tail tissues in F0 *Xenopus laevis* with an *ER^{T2}-Cre-ER^{T2}/loxP* system. (A) Overview of the transgenesis workflow. The schematic illustration of the plasmids containing the CAGGs:*ERCreER* and the CAGGs:*lp-Cherry* cassettes is indicated at the top. A summary of the result is indicated at the right side of each step. (B) Expression of nuclear TFP in the tail region of a transgenic F0 tadpole. Top: schematic illustration of a stage 49 tadpole. The red box indicates the field of view of the bottom row images. Bottom row: whole mount fluorescence images showing TFP signals in a transgenic positive tadpole (left) and a transgenic negative, stage-comparable sibling (right). The white boxes indicate the field of view of the bottom row images. Scale bars represent 200 μm. (C) Scatter plot showing the transgenic efficiencies. Each dot represents an independent REMI experiment, and the lines represent the average efficiency of two different constructs, CAGGs:*TFPnl*s (71.8%, *n* = 3) and CAGGs:*ERCreER* (4.9%, *n* = 4). The efficiency was calculated as the number of fluorescence-positive tadpoles divided by the total number surviving tadpoles. Statistical analysis was performed by one-way ANOVA and the Šidák multiple comparison test. ***p* < .01. Data are represented as mean ± SD. (D) Conditional mCherry expression in the tail region of a transgenic F0 tadpole. Top: a schematic illustration of the 4OHT treatment (black bar) and screening regime. The red boxes indicate the field of view of the middle and bottom row images. Middle row: whole mount fluorescent images of a TFP-positive tadpole before (left, Day 0) and after (right, Day 5) an overnight 4OHT treatment. The mCherry signal in the tail region was detected at Day 5. The white dashed lines outline the tail. Scale bars represent 500 μm

low transgenic efficiency, an induced mCherry signal was observed throughout the tail of all TFP-positive tadpoles 5 days after an overnight 4OHT treatment at stage 49 (Figure 1D). This result confirms that conditional labeling induced by 4OHT can be achieved at the tadpole stages.

3.2 | Conditional labeling in F1 CAGGs:ERCreER transgenic *Xenopus* lines

To determine if the convertibility of the reporter cassette could be inherited, three of the eight CAGGs:ERCreER founders were raised

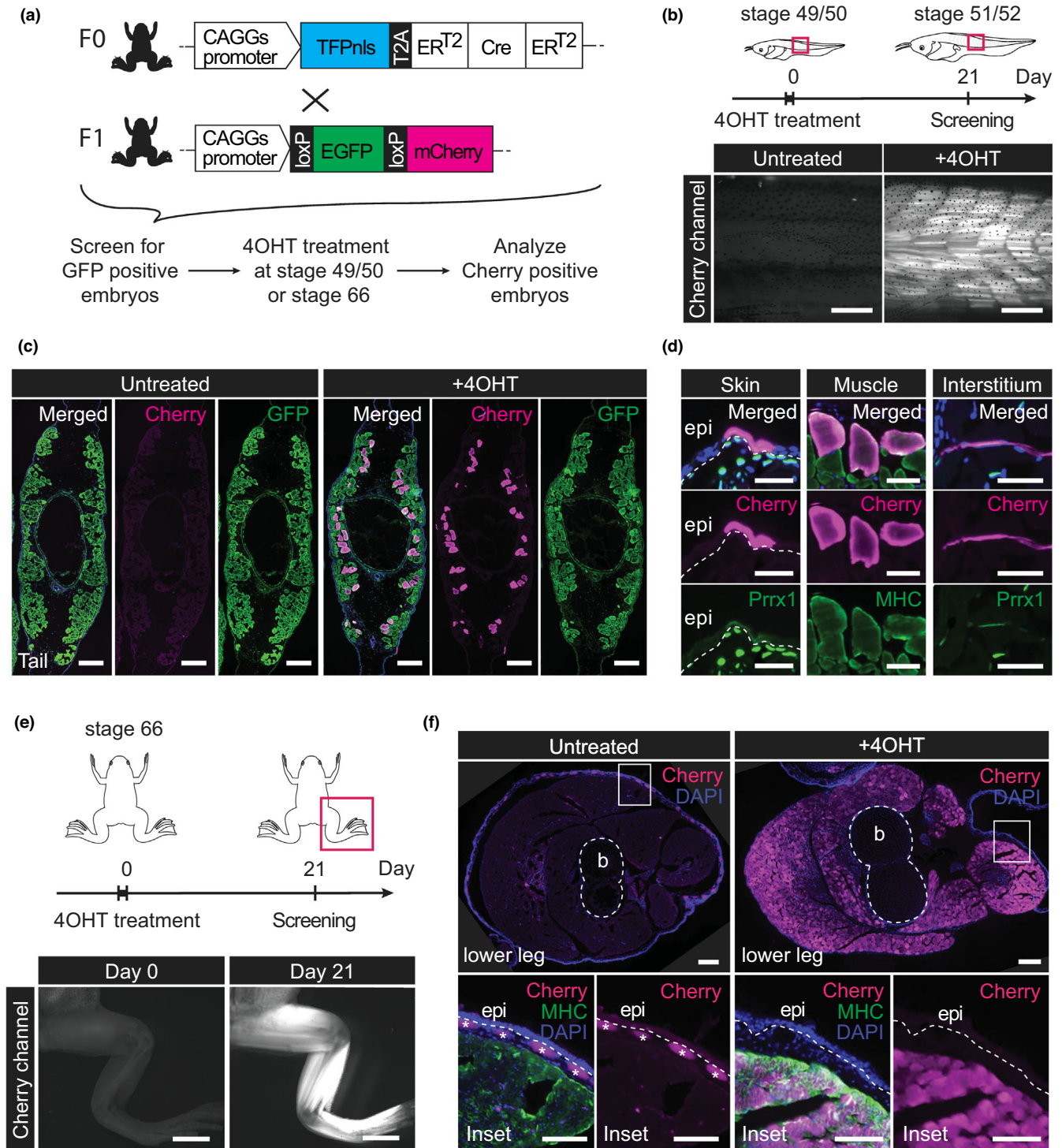


FIGURE 2 Legend on next page.

until sexual maturity and mated with the CAGGs:*lp-Cherry* reporter lines (Lin et al., 2021). Because we were not able to distinguish GFP-single positive and GFP/TFP-double positive animals by fluorescence signals, we treated all GFP-positive embryos with 4OHT at stage 49 and screened for embryos that express mCherry (Figure 2A). As expected, we observed 4OHT-induced mCherry expression in the tail tissues of the F1 progeny (Figure 2B). The CAGGs:*ERCreER*/CAGGs:*lp-mCherry*-double positive F1 animals were identified by genotyping and subsequently used for immunohistochemistry (IHC) analysis (Figure S1B). Notably, all *CreER*-positive animals contained CAGGs:*Stop-lp-Cherry* cassettes, suggesting that the mCherry signal might come from both CAGGs:*Stop-lp-Cherry* and CAGGs:*lp-Cherry* cassettes (Figure S1B). IHC analysis of the tail tissue showed that labeled cells were found in the epidermis in the skin region, muscle bundles, and interstitial cells (Figure 2C,D). In a parallel experiment where we established transgenic lines with the single *ER^{T2}* version to control Cre activity (CAGGs:*CreER*), we observed 4OHT-independent mCherry expression in the tail (Figure S1C). This result is consistent with a previous finding showing that single *ER^{T2}* was not able to block Cre activity when the cassette was driven by the CMV promoter (Werdien et al., 2001).

Despite the induction of an mCherry signal in the tail after 4OHT administration at stage 49, the same animals did not have apparent mCherry expression in the limb buds and legs (Figure S2A). Even with three consecutive pulses of 4OHT treatment before stage 49, we were not able to label limb bud cells in the CAGGs:*ERCreER* lines (data not shown). This was not due to a lack of loxP reporter in the limb as we detected GFP expression in the limb tissues (Figure S2B) and were able to label limb cells using a different promoter (see below). We suspect that the activity of the CAG promoter was low in the stage 49 limb bud so that the Cre activity was below the conversion threshold. Due to the lack of an anti-TFP antibody, we could not verify the TFP expression in the

early limb buds. In contrast, we were able to induce mCherry expression when treating the siblings with 4OHT at stage 66 (froglet stage) (Figure 2E). IHC analysis of the leg samples showed that the mCherry signal was mostly, if not completely, located in the muscle tissue (Figure 2F). Overall, this result demonstrates a proof-of-principle example that temporal control with the *Cre-ER^{T2}/loxP* system could be achieved in stable transgenic *Xenopus* lines.

3.3 | Establishing *Prrx1:CreER* transgenic lines

Next, we investigated whether we could achieve tissue-specific labeling using the *Cre-ER^{T2}/loxP* system in stable transgenic *Xenopus* lines. Our goal was to label and trace limb connective tissue cells during limb regeneration in *Xenopus* (Lin et al., 2021). To do so, we used the *mPrrx1* enhancer to drive the expression of the *Cre-ER^{T2}* cassette. The *mPrrx1* enhancer was shown to be active in the limb mesenchyme of multiple species, including *X. laevis* (Gerber et al., 2018; Logan et al., 2002; Martin & Olson, 2000; Suzuki et al., 2007). Specifically, a previous work established that the *mPrrx1* enhancer was able to drive connective tissue-specific *Cre-ER^{T2}* expression in axolotls (Gerber et al., 2018). It is worth noting that here we describe the single *ER^{T2}-Cre* (*Cre-ER^{T2}*) version instead of the double *ER^{T2}* one used above (see below and Section 4).

When we performed transgenesis with the *Prrx1:CreER* plasmid, we observed very faint TFP expression in the early limb bud to an extent that we could not efficiently distinguish TFP-positive embryos from the wild type (data not shown). To circumvent this problem, two additional adjustments were made. First, we optimized the *TFPnl5-T2A-Cre-ER^{T2}* sequence based on the codon usage preference of *X. laevis* to boost the translation of the *Cre-ER^{T2}* protein. Second, a *γ-crystallin* (*cryg1*) promoter-driven *mCherry* cassette was added in a

FIGURE 2 Conditional labeling in stable transgenic *Xenopus laevis* lines. (A) Overview of the screening procedure of the F1 CAGGs:*ERCreER* tadpoles. The schema on the top indicates the parental genotypes. (B) Conditional mCherry expression in the tail region of an F1 tadpole. Top: schematic illustration of the 4OHT treatment and screening regime. The red boxes indicate the field of view of the bottom row images. Bottom row: whole mount fluorescent images of a tadpole without (left, Untreated) and with (right, +4OHT) an overnight 4OHT treatment. The mCherry signal in the tail region was screened at Day 21. Scale bars represent 500 μ m. (C) Immunohistochemistry analysis of the conditional mCherry expression in F1 tadpoles. Cross-sections of untreated (left, Untreated) and 4OHT-converted (right, +4OHT) F1 tadpole tails were stained with anti-Cherry (magenta) and anti-GFP (green) antibodies. Nuclei were stained with DAPI (blue) and are shown in the merged image. Cherry signals were found only after 4OHT treatment. Scale bars represent 100 μ m. (D) Immunohistochemistry analysis of Cherry expression in different tail tissues after 4OHT treatment. Skin tissue (left column): Cherry (magenta)-positive and *Prrx1* (green)-negative cells were found in the epidermis. The white dashed line indicates the boundary between the dermis the epidermis (epi). Muscle tissue (middle column): Cherry (magenta)/MHC (green)-double positive muscle bundles were found in the muscle region. Interstitial tissue (right column): Cherry (magenta)/*Prrx1* (green)-double positive cells were found in the interstitial region. Nuclei were stained with DAPI (blue) and are shown in the merged images. Scale bars represent 50 μ m. (E) Conditional mCherry expression in the leg of a stage 66 F1 froglet. Top: schematic illustration of the 4OHT treatment (black bar) and screening regime. The red boxes indicate the field of view of the bottom row images. Bottom row: whole mount fluorescent images of a TFP-positive tadpole before (left, Day 0) and after (right, Day 21) an overnight 4OHT treatment. Scale bars represent 2 mm. (F) Immunohistochemistry analysis of the conditional mCherry expression in the legs of F1 froglets. Top row: cross-sections of the lower leg region of an untreated (left) and a stage-comparable 4OHT-converted (right) F1 froglet were stained with anti-Cherry (magenta) antibody and DAPI (blue). The white dashed circles indicate the bone region (b). The white boxes indicate the field of view of the bottom row images. Bottom row: the inset images of the top row. Anti-MHC staining (green) was performed to indicate the muscle bundles. Cherry signals were found in the muscle bundles after the 4OHT treatment. The white dashed lines indicate the boundary between dermis and epidermis (epi). White asterisks indicate the autofluorescence signals from gland cells. Scale bars represent 200 μ m (top row) and 100 μ m (bottom row)

reversed orientation upstream to the *mPrrx1* enhancer as a second screening marker (Figure 3A). The *cryg1:mCherry;mPrrx1:TFPnl5-T2A-Cre-ER^{T2}* plasmid (hereafter abbreviated as *Prrx1:CreER*) was used to generate transgenic founders.

Eleven lens-Cherry-positive F0 animals were raised until sexual maturity and mated with the CAGGs:*lp-Cherry* reporter lines. When treating the lens-mCherry/trunk-GFP-double positive F1s with

4OHT at stage 49, we observed 4OHT-dependent mCherry expression in the limb bud in embryos from nine out of the 11 founders. Out of the nine founders, we identified one founder (*Prrx1:CreER-F0-#2*) that had robust mCherry expression in the limb bud but not in the tail (Figure S3A). The F1 transgenic lines derived from the *Prrx1:CreER-F0-#2* founder were further characterized and are described below.

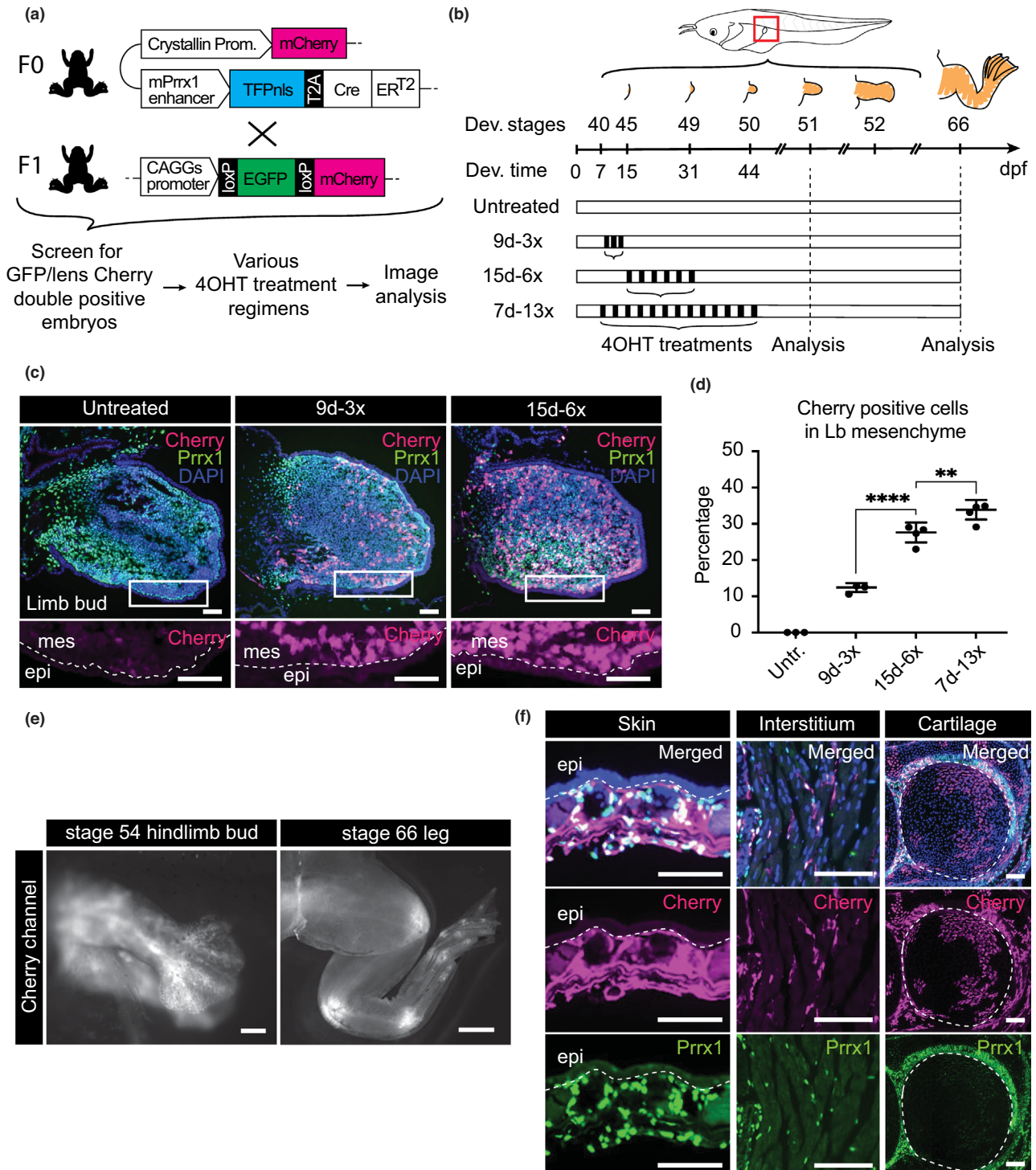


FIGURE 3 Legend on next page.

3.4 | Conditional labeling of limb connective tissue cells

To find the effective labeling timing, we first performed an overnight 4OHT treatment at stage 47 (st47T-1x), stage 52 (st52T-1x), or stage 66 (st66T-1x) and assessed mCherry expression at the froglet stage (Figure S3B). An overnight DMSO treatment at stage 47 (st47D-1x) was used as a negative control for the st47T-1x samples. mCherry expression was observed in st47T-1x, but not in st47D-1x, suggesting that the conversion was specific to 4OHT treatment (Figure S3C, upper panels). mCherry expression was strong in the st47T-1x samples and drastically weaker in the st52T-1x and st66T-1x samples, indicating a narrow window in the early development for effective 4OHT-induced cell labeling (Figure S3C).

To find the optimal cell labeling strategy, we performed three 4OHT treatment regimens during early development and determined the conversion efficiency by the mCherry signal in the stage 51 limb buds (Figure 3A,B). In agreement with a previously published result (Lin et al., 2021), three overnight 4OHT treatments starting from 9 days post-fertilization (dpf) (9d-3x) labeled $12\% \pm 1.2\%$ of the limb bud mesenchymal cells, compared to 0.0% in the control limb buds (untreated). Six 4OHT treatments starting from 15 dpf (15d-6x) increased the efficiency to $29.9\% \pm 2.7\%$. The efficiency was further increased to $32.9\% \pm 2.7\%$ when embryos were treated 13 times with 4OHT starting from 7 dpf (7d-13x) (Figure 3C,D). The more-than-doubled amount of 4OHT treatments only labeled 3% more cells, suggesting that 15–31 dpf was the critical time window to label limb cells.

Upon examining the tadpoles after the 4OHT treatment, we observed an apparent 4OHT-induced mCherry signal in the limb bud and in the brain region (Figure S4A). The mCherry signal remained in the leg throughout metamorphosis and was most obvious in the joint

regions (Figure 3E). This pattern was reminiscent of the labeling pattern of a previously reported *Prrx1:CreER* axolotl line (Gerber et al., 2018). IHC analysis showed that Cherry-positive cells were found in the dermal, interstitial, and cartilage regions as previously reported (Figure 3F) (Lin et al., 2021). It is worth noting that the 4OHT treatments were at the early embryonic stages, and the IHC analysis was done after metamorphosis. Therefore, the labeled cells may turn down *prrx1* expression when they differentiated into different cell types. An example is the *Prrx1*-negative/Cherry-positive cartilage cells showed in Figure 3F. We did not find labeled cells in the epidermis (Figure 3C,F).

Unexpectedly, some leg muscle cells were labeled in many animals upon inspection in the froglet stage (stage 66). The pattern of the labeled muscle cells varies not only between animals, but also between left and right legs (Figure S4B). It remains unclear whether it was due to an artifact of the *mPrrx1* enhancer activity, a sporadic fusion of limb connective tissue cells with muscle cells, or a reflection of the endogenous *Prrx1* activity in the frog leg muscle tissue. Interestingly, two recent studies confirmed the existence of a connective tissue/muscle dual identity cell population at the muscle tendon junction in both mice and chicken (Esteves de Lima et al., 2021; Yaseen et al., 2021). It is likely that our *Prrx1:CreER* lines labeled such population in *Xenopus* legs. To be on the safe side, leg samples that had extensive muscle labeling were excluded from downstream analysis, such as the single-cell RNA-seq and cell transplantation assays in Lin et al. (2021).

It is worth noting that we also established transgenic lines that carry the double ER^{T2} version of the *Cre* cassette (*mPrrx1:TFPnlS-T2A-ER^{T2}-Cre-ER^{T2}*). However, we did not characterize these lines further because they labeled fewer cells (Figure S4C). Overall, we successfully established *Prrx1:CreER* transgenic lines that allow temporal control of tissue-specific labeling.

FIGURE 3 Conditional labeling of limb connective tissue in *Prrx1:CreER* frog lines. (A) Overview of the screening procedure of the F1 *Prrx1:CreER* tadpoles. The schema on the top indicates the parental genotype. (B) Overview of four 4OHT treatment regimens. The developmental stages and timing (days post-fertilization [dpf]) are indicated with the corresponding limb bud schema on the top. The developing limb is shaded in yellow. The red box indicates the field of view in Figure 3C. Four regimens of 4OHT treatment are indicated as Untreated, 9d-3x (three times starting from 9 dpf), 15d-6x (six times starting from 15 dpf), and 7d-13x (13 times starting from 7 dpf). The black boxes indicate each overnight 4OHT treatment. Animals were analyzed at stage 51 and stage 66. (C) Immunohistochemistry analysis of the conditional Cherry expression in limb buds under different 4OHT regimens. Top row: longitudinal sections of stage 51 limb buds from three 4OHT regimens, Untreated (left column), 9d-3x (middle column), and 15d-6x (right column), were stained with anti-Cherry (magenta) and anti-*Prrx1* (green) antibodies and DAPI (blue). The white boxes indicate the field of view in the bottom row images. Bottom row: the inset images of the top row with the Cherry channel alone. The white dashed line indicates the boundary between mesenchyme (mes) and epidermis (epi). Note that the Cherry signal is only found in the mesenchyme. Scale bars represent 50 μm . (D) Scatter plot showing the conversion efficiencies of different 4OHT regimens. The efficiencies were determined by the percentage of Cherry-positive cells in the limb bud mesenchyme. Each dot represents an independent sample, and the line represents the average efficiency of four different regimens, Untreated (Untr., 0%, $n = 3$), 9d-3x (12.1%, $n = 3$), 15d-6x (26.9%, $n = 4$), and 7d-13x (32.9%, $n = 4$). Statistical analysis was performed by one-way ANOVA and the Šidák multiple comparison test. ** $p < .01$, **** $p < .0001$. Data are represented as mean \pm SD. (E) Whole mount fluorescence images of a stage 54 limb bud (left) and a stage 66 leg (right). Scale bars represent 500 μm (left) and 5 mm (right). (F) Immunohistochemistry analysis of the Cherry expression in different leg tissues after 4OHT treatment. Skin tissue (left column): Cherry (magenta)/*Prrx1* (green)-double positive cells were found in the dermis. The white dashed line indicates the boundary between the dermis and the epidermis (epi). Interstitial tissue (middle column): Cherry (magenta)/*Prrx1* (green)-double positive cells were found in the interstitial region. Cartilage tissue (right column): patches of Cherry (magenta)-positive cells were found in the cartilage region, which was identified by its morphology and circled by the white dashed line. Cherry (magenta)/*Prrx1* (green)-double positive perichondrium cells were also found at the boundary of cartilage. Nuclei were stained with DAPI (blue) and are shown in the merged images on the top row (Merged). Scale bars represent 100 μm

3.5 | Conditional labeling of other organs in *Prrx1:CreER* frog lines

In addition to having activity in the limb mesenchyme, the *mPrrx1* enhancer has been shown to have activities in the maxillary process and brain regions (Martin & Olson, 2000). We observed mCherry signals in the brain regions of the 4OHT-treated stage 50 tadpoles (Figures 4A and S4A). IHC analysis showed Cherry expression in the midbrain region (Figure 4B). Specifically, we found Cherry-positive cells in the ventricular layer, where the ependymal cells reside. Trails of Cherry-positive cells were commonly found stemming from the ventricular cell layer extending outward, suggesting that our *Prrx1:CreER* lines labeled ependymal cells and their neuronal descendants.

Although mCherry expression in other organs was not obvious in the whole mount image (Figure S3A), IHC analysis showed Cherry-positive cells in the head and tail dermis (Figure 4C,D) and fin mesenchyme (Figure 4E). We also found few Cherry-positive cells in the heart and spinal cord tissues (Figure S5A,B), although the exact origin of those cells remains to be determined. Importantly, we did not find any Cherry-positive cells apart from the lens in the untreated controls (data not shown), indicating that mCherry expression is 4OHT-dependent. It also indicated that the *cryg1* promoter only drove mCherry expression in the lens. These data suggest that our *Prrx1:CreER* lines could be valuable for future studies on those tissues and that the *Cre-ERT²/loxP* system could be applied to label cells other than limb fibroblasts.

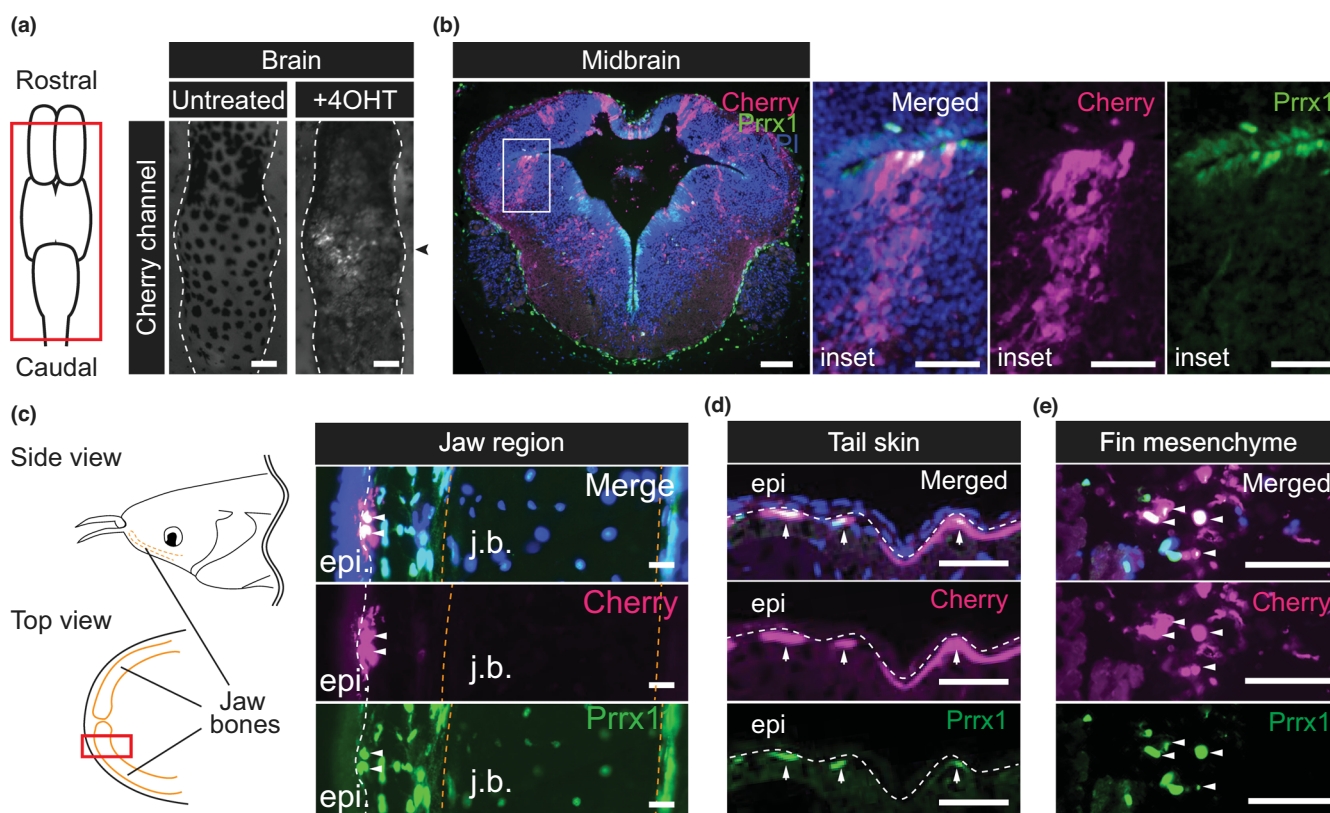


FIGURE 4 Conditional labeling of cells in other organs in *Prrx1:CreER* frog lines. (A) Conditional mCherry expression in the brain of a stage 49 tadpole. Left: schematic illustration of the overall brain structure. Top is the rostral side and bottom is the caudal side. The red box indicates the field of view of the right panel. Right: whole mount fluorescence images of the brain region of tadpoles without and with 4OHT treatment. White dashed lines outline the brain. Black arrowhead indicates the level of the section plane in (B). Scale bars represent 200 μ m. (B) Immunohistochemistry analysis of the Cherry expression in a tadpole midbrain region after 4OHT treatment. Left: a cross-section of the midbrain was stained with anti-Cherry (magenta) and anti-Prrx1 (green) antibodies and DAPI (blue). The white box indicates the field of view of the inset images on the right. Scale bars represent 100 μ m (left) and 50 μ m (inset). (C) Immunohistochemistry analysis of the Cherry expression in the head dermis of a tadpole after 4OHT treatment. Left: schematic illustrations of the jaw region viewed from the side (top panel) and from the top (bottom panel) of a tadpole. Jawbones are outlined by solid or dashed orange lines. The red box indicates the field of view in the bottom images. Bottom: a longitudinal section of the jaw region was stained with anti-Cherry (magenta) and anti-Prrx1 (green) antibodies and DAPI (blue). Cherry-positive cells were found in the dermis, expressing Prrx1 (white arrowheads). No Cherry-positive cells were found in the jawbone (j.b.). The white dashed line indicates the boundary between dermis and epidermis (epi). Orange dashed lines outline the jawbone. Scale bars represent 20 μ m. (D) Immunohistochemistry analysis of the Cherry expression in the tail dermis after 4OHT treatment. Cross-sections of the tail were stained with anti-Cherry (magenta) and anti-Prrx1 (green) antibodies and DAPI (blue). The white dashed line indicates the boundary between dermis and epidermis (epi). White arrowheads indicate the Prrx1/Cherry-double positive tail dermal cells. Scale bars represent 50 μ m. (E) Same analysis as (D) but in the fin mesenchyme region. Scale bars represent 50 μ m

4 | DISCUSSION

The *Cre-ER^{T2}/loxP* system is the most commonly used strategy to trace cells. It has been adopted in many species. We recently reported a transgenic *Xenopus* line harnessing such system (Lin et al., 2021), the details of which we described in this study. Here we discuss critical variables that we identified in making such transgenic lineage tracing system in *X. laevis*.

A significant lower transgenic efficiency was observed when generating *Cre-ER^{T2}* transgenic lines, as only 4.9% of the surviving embryos had a detectable TFP signal when using the *CAGGs:ERCReER* plasmid, compared to 71.8% when using the *CAGGs:TFPnl*s plasmid. A possible explanation is that the pan-expression of the *ER^{T2}-Cre-ER^{T2}* protein was adverse to early development so that the surviving embryos must either have a low copy number of *ER^{T2}-Cre-ER^{T2}* or silence the integrated *ER^{T2}-Cre-ER^{T2}* cassettes. Consistent with this hypothesis, we observed a low intensity of TFP signals in *CAGGs:ERCReER* animals compared to *CAGGs:TFPnl*s animals (data not shown). Alternatively, the low efficiency might also be due to the increased size of the *Cre* cassettes as we observed a negative correlation between transgenic efficiency and cassette length in general (Figure S1A). The underlying mechanism however remains to be investigated.

Choosing a suitable fluorescent marker to facilitate the screening process was crucial to identify positive embryos. We used TFP because it is 1.58-fold brighter than eGFP (Ai & Campbell, 2008) and we were able to detect the nuclear TFP signal in the tails of *CAGGs:ERCReER* animals. Of the eight TFP-positive embryos identified, all showed robust 4OHT-induced mCherry expression in the tail. On the other hand, we were not able to unambiguously identify TFP signals in the hindlimb bud in the case of *Prrx1:CreER* experiments. This is likely due to the combination of low transgene expression and the auto-fluorescent nature of the *Xenopus* limb bud tissue in the blue and green channels. The addition of the lens marker helped tremendously in that regard. A caveat for this method was that lens-mCherry expression did not reflect the in situ *Cre-ER^{T2}* expression because they were driven by different promoters. This explained the fact that only the progenies from one of the nine *Prrx1:CreER* founders had robust and specific mCherry expression in the limb bud mesenchyme even though they all have mCherry-positive lenses. For generating new transgenic lines in the future, one might consider using different fluorescent proteins that have a longer emission wavelength to circumvent this issue.

The presence of *ER^{T2}* controls the distribution of *Cre* protein between the cytosol and the nuclei in an equilibrium state, and the recombination of chromosomes likely happens when the nuclear protein levels of *Cre* protein reach a certain threshold value. Therefore, to achieve stringent but robust cell labeling, it is important to consider the balance between promoter strength and the number of *ER^{T2}* used in the system. For example, when pairing the single *ER^{T2}* version of *Cre* (*CreER*) with a strong promoter, such as the *CAG* promoter, we observed mCherry expression without 4OHT treatment (Figure S1B). The “leaky” conversion of the *CAGGs:CreER* lines was likely due to the

over-the-threshold *Cre* activity in the nuclei resulting from the high copy number of *Cre-ER^{T2}* protein. In the case of the double *ER^{T2}* version (*ERCReER*), the equilibrium shifts toward the cytosol and the recombination threshold was not reached due to the lower basal level of *Cre* protein in the nucleus in the homeostatic state. However, the control of double *ER^{T2}* might be too “tight” when the *Cre-ER^{T2}* cassette is driven by other promoters. For instance, when pairing the *ER^{T2}-Cre-ER^{T2}* cassette with the *mPrrx1* enhancer, we could only label few cells in the limb (Figure S4C). Unfortunately, whether it is better to use the single or double *ER^{T2}* version has to be determined empirically at the moment. Investigating the relationship between the recombination threshold and the copy number of *Cre* protein could help to reduce the time and effort to establish *Cre-ER^{T2}* transgenic *Xenopus* lines in the future.

Our data show that the timing of 4OHT administration is crucial to label leg cells. Bathing *CAGGs:ERCReER* tadpoles in 4OHT at stage 49 labeled tail tissues, but not leg tissues (Figure S2A). However, the leg cells could be labeled when the animals of the same batch were treated with 4OHT at the froglet stage (Figure 2E). On the other hand, 4OHT treatment must be given before the onset of limb bud development when using the *mPrrx1* enhancer to achieve robust cell labeling in the limb mesenchyme (Figure S3C). Therefore, identifying the optimal 4OHT treatment regime for individual promoters is not trivial. A previous attempt to label leg muscle tissue with a split-*Cre* system only labeled tail muscles but not leg muscles (Rodrigues et al., 2012). In that study, one part of the *Cre* protein was controlled by a heat shock promoter and the other part by a cardiac actin promoter. We suspect that the reason why the leg muscle was not labeled was because the heat shock activation was done before the onset of the limb bud development (2–4 weeks after birth).

Our work shows that *Cre-ER^{T2}/loxP*-mediated conditional and tissue-specific cell labeling could be used to establish stable transgenic *Xenopus* lines. In the future, one could consider using the CRISPR/Cas9 method to knock in the *Cre-ER^{T2}* cassette to a genomic locus of interest. Although it remains to be determined whether a single copy of the transgene would be enough to achieve robust *Cre-ER^{T2}/loxP*-mediated cell labeling in *Xenopus*, such method has been successfully used in axolotls (Fei et al., 2017). The expression pattern of the *Cre-ER^{T2}* cassette would better reflect the expression pattern of the endogenous gene of interest, without the need of a pre-characterized promoter. This feature would open the door to trace cells based on the expression of literally any gene. To sum up, we hope that the present study will serve as a reference and encourage researchers to establish *Xenopus* lines that are suitable for lineage tracing.

AUTHOR CONTRIBUTIONS

TY.L. and S.H. generated transgenic *X. laevis* lines with assistance from P.M. and Y.T.S. TY.L. designed and performed the experiments. TY.L. and E.M.T. analyzed data and wrote the manuscript.

ACKNOWLEDGMENTS

We thank the animal care team at the Vienna BioCenter and CRTD Dresden for great animal care and breeding, and all the members of

the Tanaka lab for helpful discussions. We thank Nicole Ziegler and Eva Kania for technical assistance. The *X. laevis cryg1* promoter sequence was kindly provided by Professor Daniel L. Weeks in the Department of Biochemistry, University of Iowa. We thank Keisuke Ishihara for the critical comments on the manuscript. We thank the VBCF NGS facility and the IMP Bio-Optics and MBS facilities for outstanding service. Animal experiments were performed as approved by the Magistrate of Vienna and the State Authorities Saxony.

CONFLICT OF INTERESTS

The authors declare that there is no conflict of interests.

ORCID

Tzi-Yang Lin  <https://orcid.org/0000-0001-6443-7760>

Prayag Murawala  <https://orcid.org/0000-0002-0607-1059>

Elly M. Tanaka  <https://orcid.org/0000-0003-4240-2158>

REFERENCES

- Ai, H. W., & Campbell, R. E. (2008). Teal fluorescent proteins: Characterization of a reversibly photoswitchable variant. *Small Animal Whole-Body Optical Imaging Based on Genetically Engineered Probes*, 6868, 6868OD. <https://doi.org/10.1117/12.761423>
- Esteves de Lima, J., Blavet, C., Bonnin, M. A., Hirsinger, E., Comai, G., Yvernogeu, L., ... Duprez, D. (2021). Unexpected contribution of fibroblasts to muscle lineage as a mechanism for limb muscle patterning. *Nature Communications*, 12(1), 3851. <https://doi.org/10.1038/s41467-021-24157-x>
- Fei, J. F., Schuez, M., Knapp, D., Taniguchi, Y., Drechsel, D. N., & Tanaka, E. M. (2017). Efficient gene knockin in axolotl and its use to test the role of satellite cells in limb regeneration. *Proceedings of the National Academy of Sciences of the United States of America*, 114(47), 12501–12506. <https://doi.org/10.1073/pnas.1706855114>
- Feil, R., Wagner, J., Metzger, D., & Chambon, P. (1997). Regulation of Cre recombinase activity by mutated estrogen receptor ligand-binding domains. *Biochemical and Biophysical Research Communications*, 237(3), 752–757. <https://doi.org/10.1006/bbrc.1997.7124>
- Gerber, T., Murawala, P., Knapp, D., Masselink, W., Schuez, M., Hermann, S., ... Treutlein, B. (2018). Single-cell analysis uncovers convergence of cell identities during axolotl limb regeneration. *Science*, 362(6413), eaaq0681. <https://doi.org/10.1126/science.aaq0681>
- Hans, S., Kaslin, J., Freudenreich, D., & Brand, M. (2009). Temporally-controlled site-specific recombination in zebrafish. *PLoS One*, 4(2), e4640. <https://doi.org/10.1371/journal.pone.0004640>
- Khattak, S., Schuez, M., Richter, T., Knapp, D., Haigo, S. L., Sandoval-Guzman, T., ... Tanaka, E. M. (2013). Germline transgenic methods for tracking cells and testing gene function during regeneration in the axolotl. *Stem Cell Reports*, 1(1), 90–103. <https://doi.org/10.1016/j.stemcr.2013.03.002>
- Kroll, K. L., & Amaya, E. (1996). Transgenic *Xenopus* embryos from sperm nuclear transplantations reveal FGF signaling requirements during gastrulation. *Development*, 122(10), 3173–3183. <https://www.ncbi.nlm.nih.gov/pubmed/8898230>
- Lin, T. Y., Gerber, T., Taniguchi-Sugiura, Y., Murawala, P., Hermann, S., Grosser, L., ... Tanaka, E. M. (2021). Fibroblast dedifferentiation as a determinant of successful regeneration. *Developmental Cell*, 56(10), 1541–1551 e1546. <https://doi.org/10.1016/j.devcel.2021.04.016>
- Logan, M., Martin, J. F., Nagy, A., Lobe, C., Olson, E. N., & Tabin, C. J. (2002). Expression of Cre recombinase in the developing mouse limb bud driven by a Pxl enhancer. *Genesis*, 33(2), 77–80. <https://doi.org/10.1002/gene.10092>
- Martin, J. F., & Olson, E. N. (2000). Identification of a prx1 limb enhancer. *Genesis*, 26(4), 225–229. <https://www.ncbi.nlm.nih.gov/pubmed/10748458>, <https://onlinelibrary.wiley.com/doi/pdfdirect/10.1002/%28SICI%291526-968X%28200004%2926%3A4%3C225%3A%3AAID-GENE10%3E3.0.CO%3B2-F?download=true>
- Metzger, D., & Chambon, P. (2001). Site- and time-specific gene targeting in the mouse. *Methods*, 24(1), 71–80. <https://doi.org/10.1006/meth.2001.1159>
- Nieuwkoop, P. D., & Faber, J. (1956). *Normal table of Xenopus laevis (Daudin); a systematical and chronological survey of the development from the fertilized egg till the end of metamorphosis*. North-Holland Pub. Co.
- Rodrigues, A. M., Christen, B., Marti, M., & Izpisua Belmonte, J. C. (2012). Skeletal muscle regeneration in *Xenopus* tadpoles and zebrafish larvae. *BMC Developmental Biology*, 12, 9. <https://doi.org/10.1186/1471-213X-12-9>
- Sive, H. L., Grainger, R. M., & Harland, R. M. (2000). *Early development of Xenopus laevis: A laboratory manual*. Cold Spring Harbor Laboratory Press.
- Suzuki, M., Satoh, A., Ide, H., & Tamura, K. (2007). Transgenic *Xenopus* with prx1 limb enhancer reveals crucial contribution of MEK/ERK and PI3K/AKT pathways in blastema formation during limb regeneration. *Developmental Biology*, 304(2), 675–686. <https://doi.org/10.1016/j.ydbio.2007.01.019>
- Werdien, D., Peiler, G., & Ryffel, G. U. (2001). FLP and Cre recombinase function in *Xenopus* embryos. *Nucleic Acids Research*, 29(11), E53–E553. <https://doi.org/10.1093/nar/29.11.e53>
- Yaseen, W., Kraft-Sheleg, O., Zaffryar-Eilot, S., Melamed, S., Sun, C., Millay, D. P., & Hasson, P. (2021). Fibroblast fusion to the muscle fiber regulates myotendinous junction formation. *Nature Communications*, 12(1), 3852. <https://doi.org/10.1038/s41467-021-24159-9>

SUPPORTING INFORMATION

Additional supporting information may be found in the online version of the article at the publisher's website.

How to cite this article: Lin, T.-Y., Taniguchi-Sugiura, Y., Murawala, P., Hermann, S., & Tanaka, E. M. (2022). Inducible and tissue-specific cell labeling in *Cre-ER^{T2}* transgenic *Xenopus* lines. *Development, Growth & Differentiation*, 64(5), 243–253. <https://doi.org/10.1111/dgd.12791>